

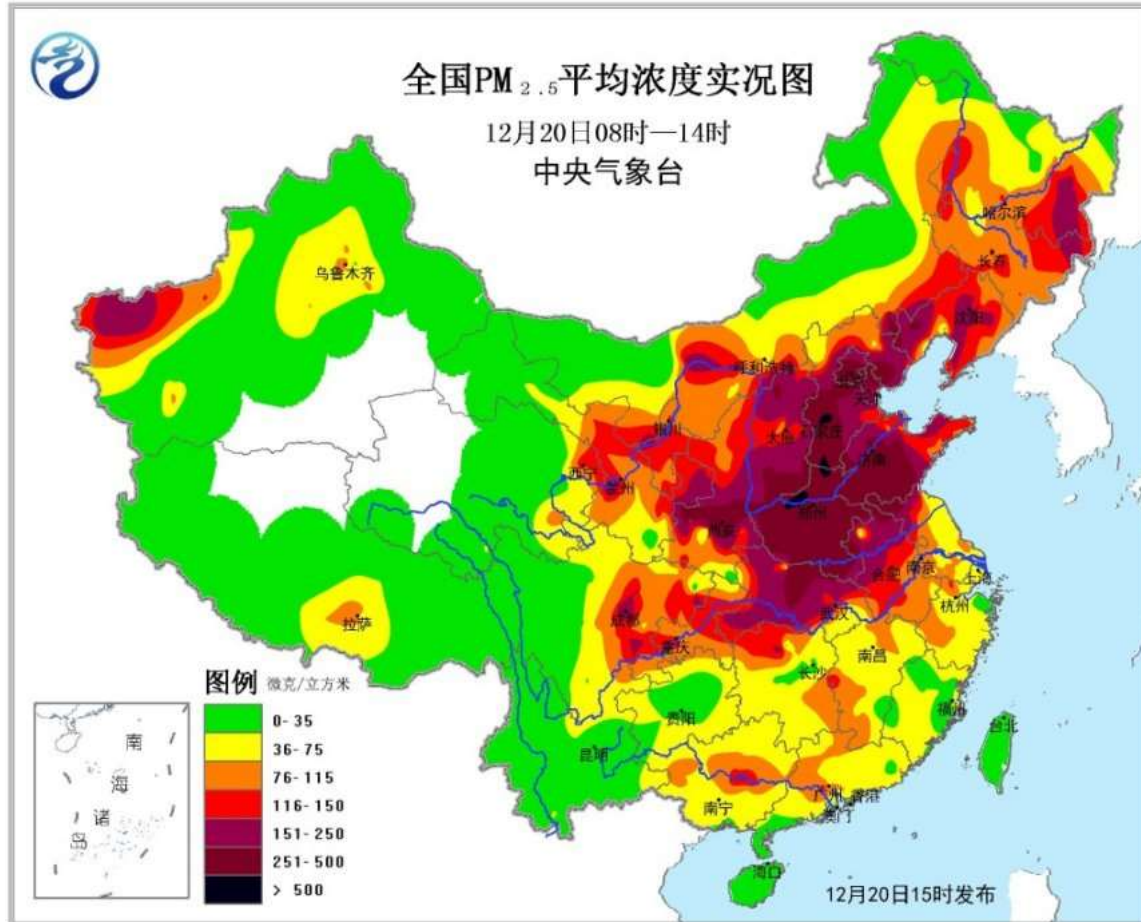
Aerosol aqueous phase oxidation of SO₂ by NO₂ in Chinese haze formation process

Gehui Wang, Jiayuan Wang, Can Wu, Jianjun Li

**School of Geographic Sciences,
East China Normal University, Shanghai, China**

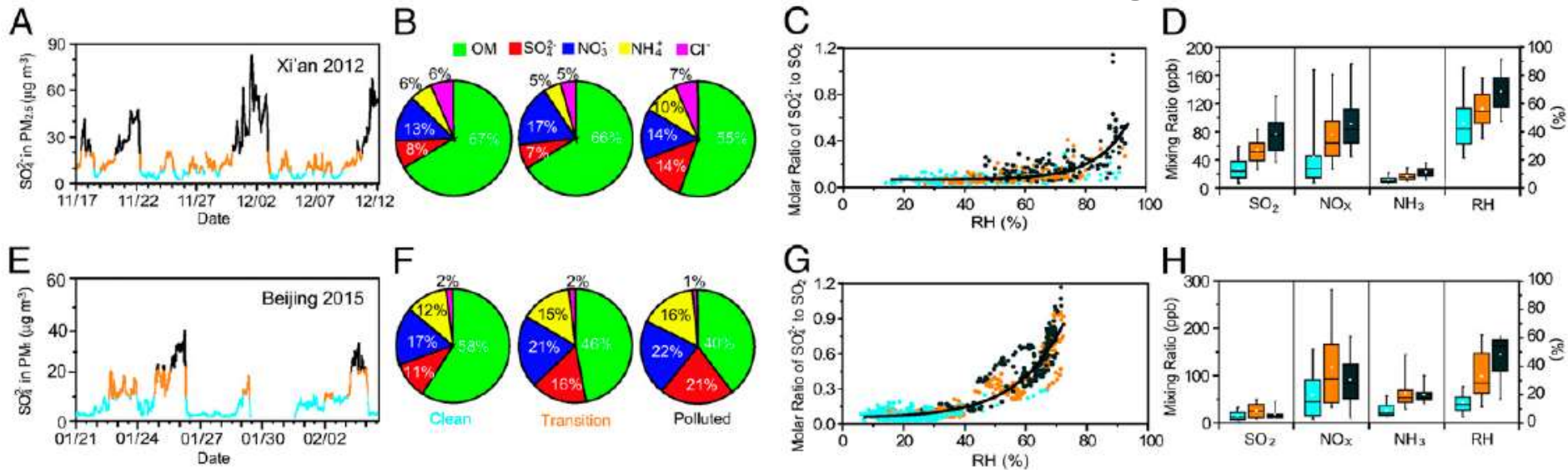
June 5-9, 2017 Guangzhou China

Hourly concentration of PM_{2.5} in China on December 20, 2016



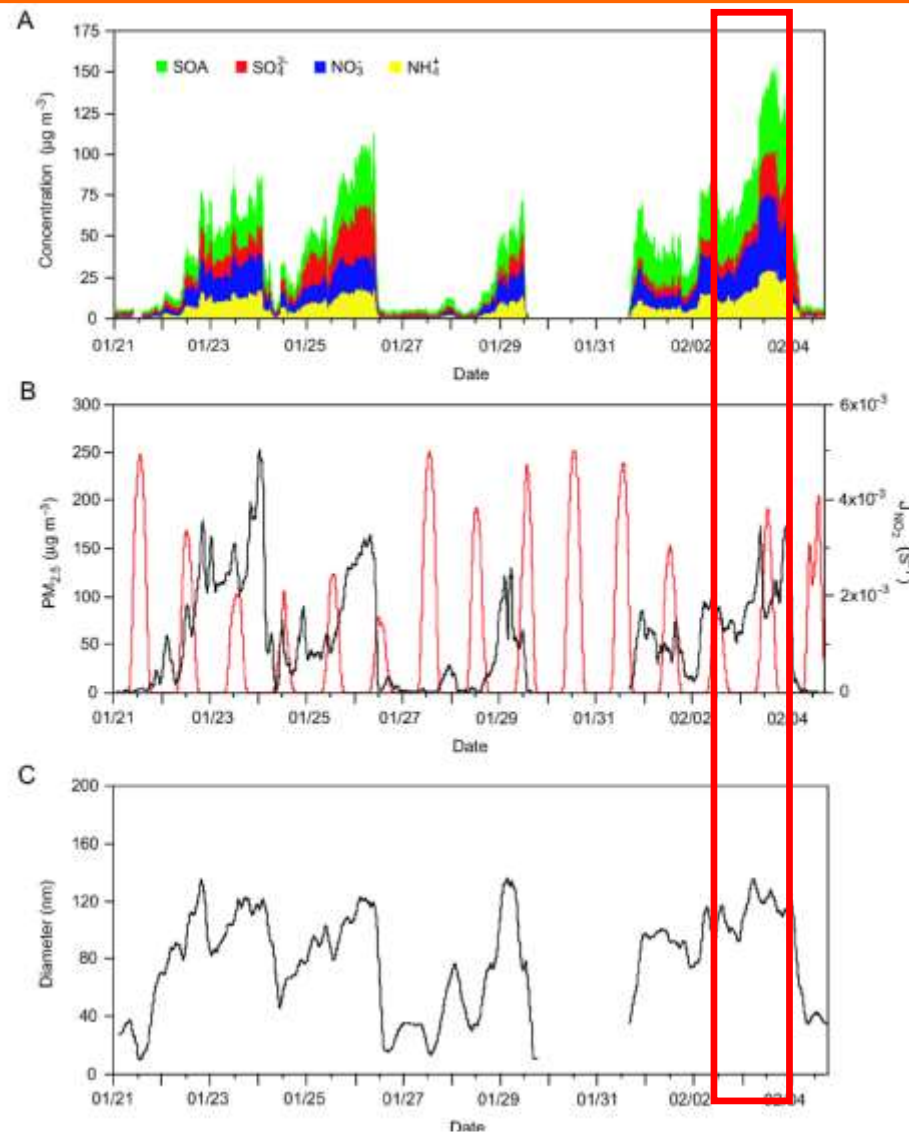
Hourly variation of sulfate in Xi'an and Beijing: Significant aqueous sulfate production

(Wang et al., PNAS 2016)

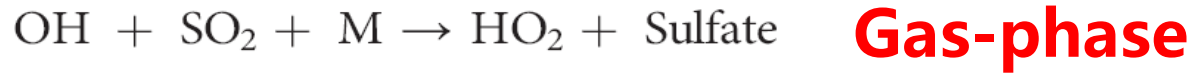


- (1) Clean period : OM (organic matter) dominant Polluted period: inorganic SNA dominant
- (2) OM in Xi'an more abundant than in Beijing
- (3) Sulfate increased exponentially with RH
- (4) Rapid conversion of SO₂ to SO₄²⁻ in Beijing under lower RH compared to that in Xi'an
- (5) High levels of SO₂, NO_x and NH₃ in haze periods along with high RH

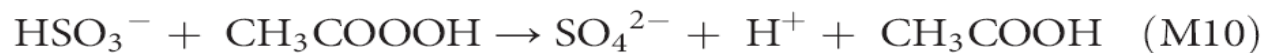
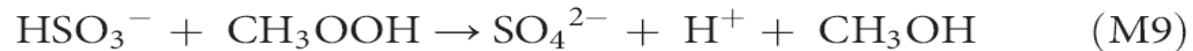
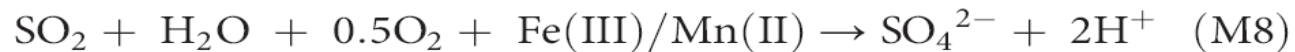
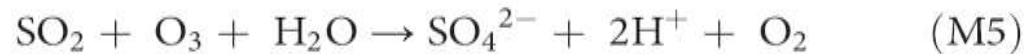
Weak photochemical activity on hazy day: low ozone, reduced visibility

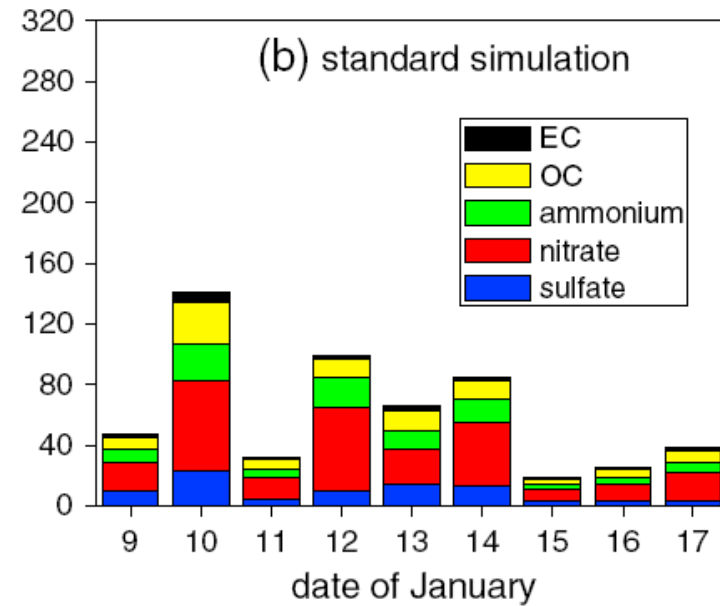
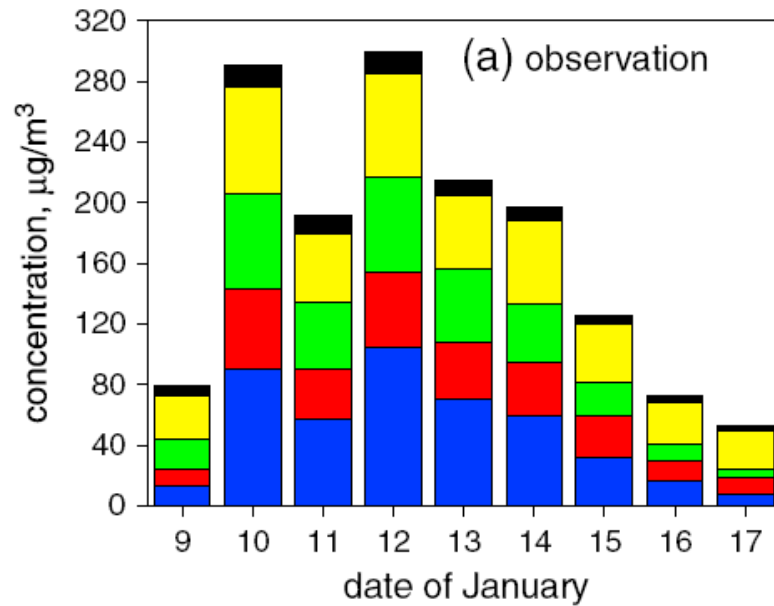


Formation mechanisms of atmospheric sulfate in models



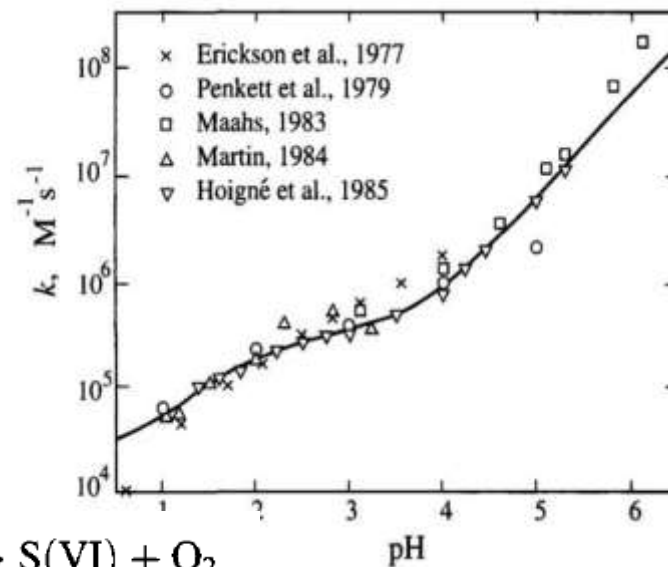
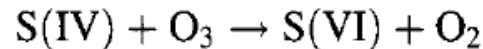
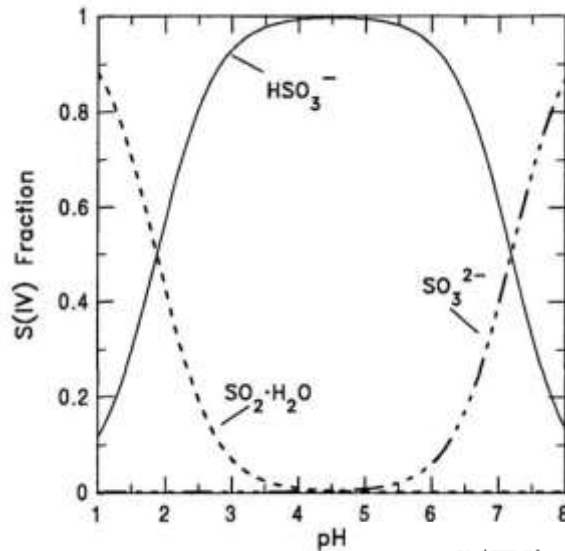
Aqueous phase



**Table 2.** A Summary of All the Simulations in This Study

Simulation Name	Description
Standard simulation	Model standard simulation with the 2013 inventory
DoubleSO ₂ run	SO ₂ emissions from the standard simulation are doubled over NC and reduced by 30% over SC. Changes are applied uniformly throughout January.
Emission_run	Total monthly emissions of SO ₂ , OC, and EC (anthropogenic portions only) from the standard run are increased by 100% over NC; SO ₂ emissions over SC are reduced by 30%; NO _x and NH ₃ emissions are the same as those in the standard run. The meteorology correction factors are applied on a day-to-day basis to emissions of SO ₂ , NO _x , NH ₃ , OC, and EC over NC.
Gamma_run T1	Emissions are the same as in the emission_run; $\gamma = 10^{-4}$ when RH = 50%, $\gamma = 10^{-3}$ when RH = 50%; γ increases linearly with RH from 50% to 100% (equation (2)).
Gamma_run T2	Emissions are the same as those in the emission_run; $\gamma = 10^{-3}$ when RH = 50%, $\gamma = 10^{-2}$ when RH = 50%; γ increases linearly with RH from 50% to 100% (equation (2)).
Gamma_run T3	Emissions are the same as those in the emission_run; $\gamma = 10^{-2}$ when RH = 50%, $\gamma = 10^{-1}$ when RH = 50%; γ increases linearly with RH from 50% to 100% (equation (2)).

Acidity is key to SO₂ oxidation in aerosol aqueous phase



$$R_0 = -\frac{d[\text{S(IV)}]}{dt} = (k_0[\text{SO}_2 \cdot \text{H}_2\text{O}] + k_1[\text{HSO}_3^-] + k_2[\text{SO}_3^{2-}])[\text{O}_3] \quad (7.80)$$

with $k_0 = 2.4 \pm 1.1 \times 10^4 \text{ M}^{-1} \text{ s}^{-1}$, $k_1 = 3.7 \pm 0.7 \times 10^5 \text{ M}^{-1} \text{ s}^{-1}$ and, $k_2 = 1.5 \pm 0.6 \times 10^9 \text{ M}^{-1} \text{ s}^{-1}$. The activation energies recommended by Hoffmann and Calvert (1985) are based on the work of Erickson et al. (1977) and are 46.0 kJ mol^{-1} for k_1 and 43.9 kJ mol^{-1} for k_2 .

- (1) When $\text{pH} > 3.0$, SO₂ almost entirely exists as HSO₃⁻, SO₃²⁻, solubility enhanced
- (2) Oxidation rate also sharply increased

Classic Textbook : SO₂ oxidation by NO₂ is unimportant

S(IV)-S(VI) TRANSFORMATION AND SULFUR CHEMISTRY 317

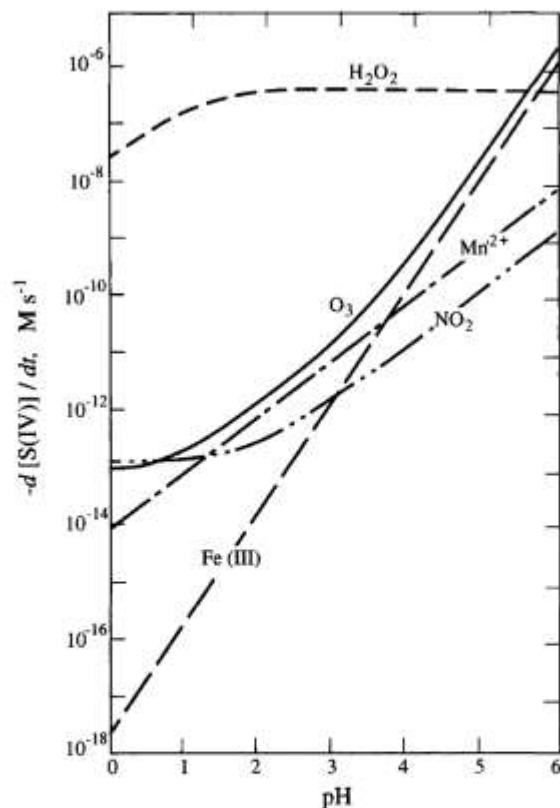
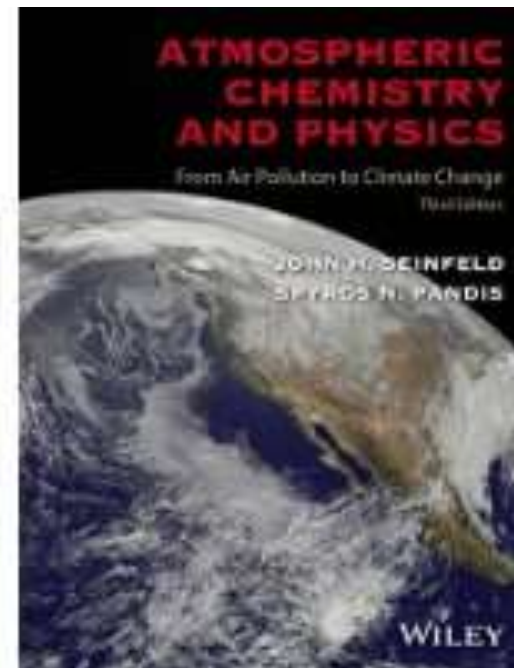


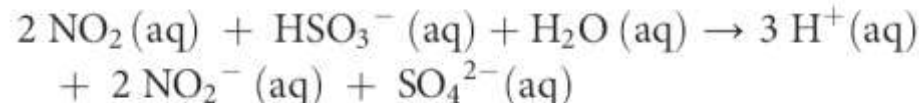
FIGURE 7.19 Comparison of aqueous-phase oxidation paths. The rate of conversion of S(IV) to S(VI) as a function of pH. Conditions assumed are [SO₂(g)] = 5 ppb; [NO₂(g)] = 1 ppb; [H₂O₂(g)] = 1 ppb; [O₃(g)] = 50 ppb; [Fe(III)] = 0.3 μM; [Mn(II)] = 0.03 μM.

oxidation rates in μM h⁻¹ for the different paths at 298 K for the conditions

[SO ₂ (g)] = 5 ppb	[H ₂ O ₂ (g)] = 1 ppb
[NO ₂ (g)] = 1 ppb	[O ₃ (g)] = 50 ppb
[Fe(III)(aq)] = 0.3 μM	[Mn(II)(aq)] = 0.03 μM



We see that under these conditions oxidation by dissolved H₂O₂ is the predominant pathway for sulfate formation at pH values less than roughly 4–5. At pH ≥ 5 oxidation by O₃ starts dominating and at pH 6 it is 10 times faster than that by H₂O₂. Also, oxidation of S(IV) by O₂ catalyzed by Fe and Mn may be important at high pH, but uncertainties in the rate expressions at high pH preclude a definite conclusion. Oxidation of S(IV) by NO₂ is unimportant at all pH for the concentration levels above.



(Y. N. Lee et al, 1983)



Transition metal ions (Fe/Mn) are negligible

Table S1. Gaseous and PM pollutants and meteorological parameters during Xi'an 2012

	Clean		Transition		Polluted	
	Mean	Range	Mean	Range	Mean	Range
I. Gaseous pollutants (ppb)						
SO ₂	28±17	1.0–86	54±22	17–191	78±31	16–203
NO _x	44±49	5.0–264	76±51	15–300	92±39	25–245
O ₃	7.4±7.0	0.0–26	4.1±4.7	0.4–11	4.1±2.4	0.6–9.6
NH ₃	12±7.4	4.7–67	17±7.7	7.6–35	23±8.3	9.3–61
HONO	1.3±1.0	0.2–5.4	2.1±1.3	0.2–6.5	2.7±1.8	0.3–10
II. Inorganic ions, Fe, Mn and organic matter in PM_{2.5} (µg m⁻³)						
SO ₄ ²⁻	5.9±2.2	2.3–10	14±4.4	10–20	38±14	20–83
NO ₃ ⁻	8.7±4.9	1.4–25	16±6.7	3.8–35	33±10	12–55
Cl ⁻	4.0±3.7	0.0–22	9.8±5.1	2.4–28	14±6.3	2.6–34
NH ₄ ⁺	4.0±2.2	0.8–11	10±3.7	5.1–18	25±7.7	3.2–44
Na ⁺	3.6±3.2	0.2–8.4	4.5±3.2	0.5–17	4.2±2.7	0.5–17
K ⁺	1.3±0.7	0.3–4.1	3.1±1.2	1.3–7.0	4.6±1.4	1.8–8.3
Mg ²⁺	0.2±0.1	0.1–0.7	0.3±0.1	0.0–0.7	0.3±0.1	0.0–0.8
Ca ²⁺	1.6±1.0	0.3–6.3	2.4±1.2	0.0–5.3	2.3±1.2	0.2–5.9
Total ions	29±13	6.8–63	60±19	34–97	121±32	65–199
Fe (µg m ⁻³)	0.82±0.29	0.37–1.13	1.51±0.70	0.60–3.0	1.76±0.66	0.79–2.79
Mn (µg m ⁻³)	0.04±0.04	0.00–0.10	0.11±0.08	0.04–0.35	0.15±0.07	0.08–0.29
Water-soluble Fe (ng m ⁻³)	1.5±2.1	0.0–6.1	4.6±3.9	0.0–14	16±5.1	7.3–23
Water-soluble Mn (ng m ⁻³)	10±2.1	3.8–20	21±8.7	11–40	41±16	17–70
Organic matter (OM)	35±15	7.0–70	99±33	38–163	177±39	116–288
pH	6.70±1.40	4.43–11.0	6.04±1.24	4.16–8.03	6.96±1.33	4.14–8.16
III. PM_{2.5} and meteorological parameters						
PM _{2.5} (µg m ⁻³)	43±18	8.0–74	139±65	76–613	250±120	101–839
T (°C)	5.7±4.1	-2.0–17	4.1±4.0	-2.3–11	4.1±4.4	-3.1–14
RH (%)	46±18	14–94	56±17	26–93	68±14	41–93
Visibility (km)	8.9±3.4	3.2–17	6.1±2.8	2.4–12	3.2±1.1	1.4–7.2

Experimental simulation : SO₂ (g) oxidation by NO₂ (g) in bulk solution

Lab experiment: in a reaction cell covered with aluminum foil (20°C)

(1) SO₂ (g) + NO₂ (g) + H₂O

(2) SO₂ (g) + NO₂ (g) + NH₃·H₂O (3%)

Table S3. Detection of sulfate formation in the reaction cell

Experimental run	SO ₂ (350 ppm)	NO ₂ (350 ppm)	Water	3 wt % NH ₃	Integrated sulfate desorption peak area (x 10 ⁶ cps)
1 (3)	In N ₂	In N ₂	√	x	6.8±2.6
2 (3)	In N ₂	In N ₂	x	√	1.0 ±4.3
3 (1)	In air	In air	√	x	6.5
4 (1)	In air	In air	x	√	10.0

The symbols “√” and “x” indicate whether a water or NH₃ solution was used and not used in the exposure, respectively. The number in parenthesis on the right column denotes the number of repeating experiments.

Results and conclusion:

(1) SO₂ can rapidly be oxidized by NO₂ into SO₄²⁻

(2) NH₃ could promote the reaction

(3) O₂ does not take an important role in the SO₂ conversion process

Smog chamber simulation : SO₂+NO₂

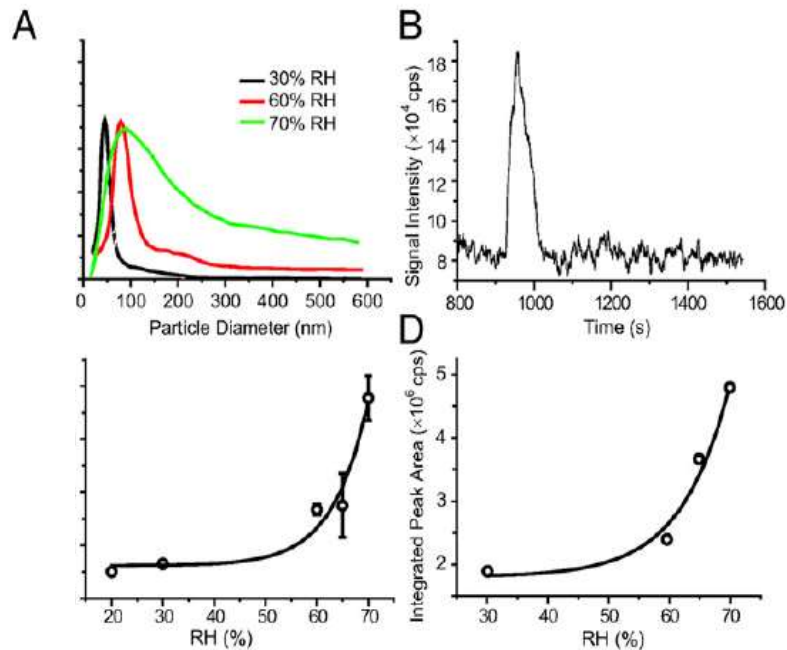
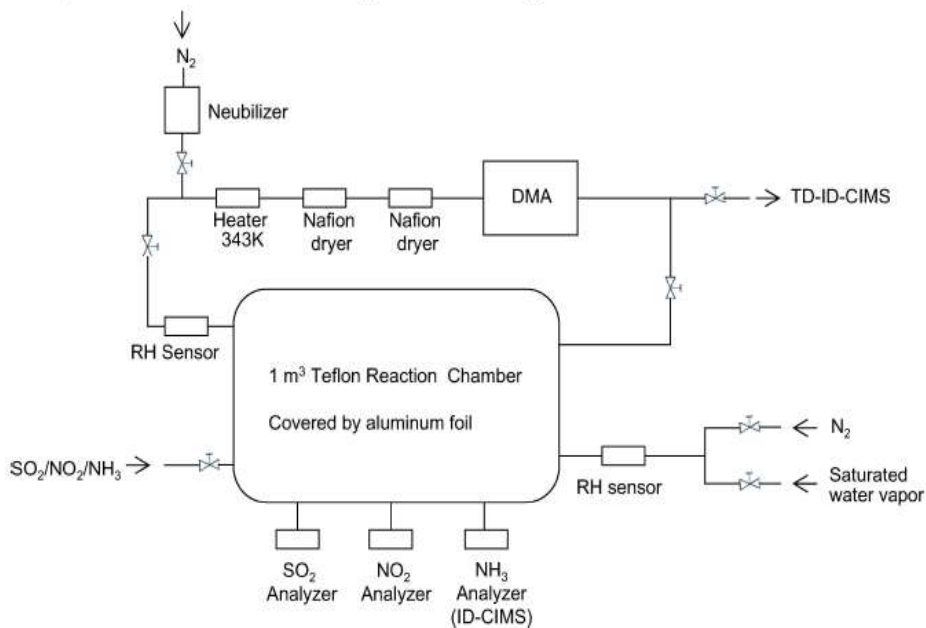
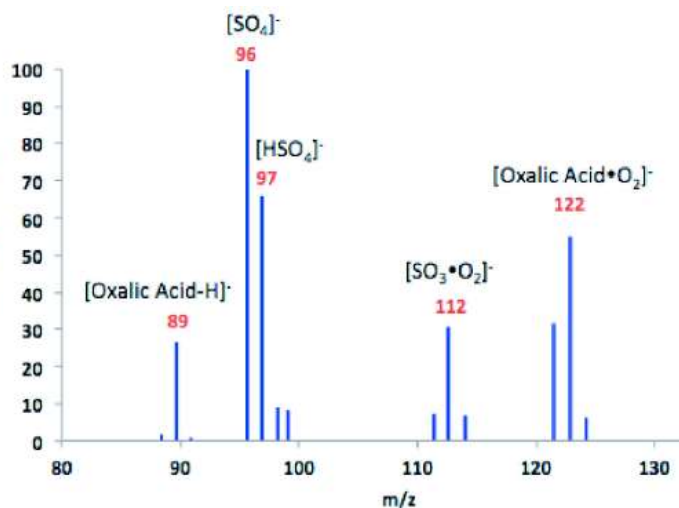
Using 1 m³ PTFE chamber covered completely with aluminium foil:

(1) 45 nm seed (oxalic acid)

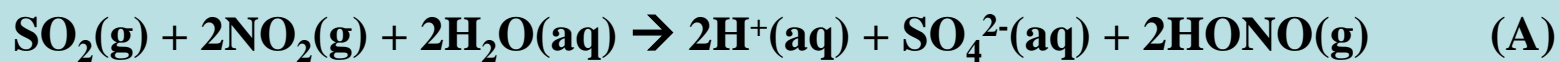
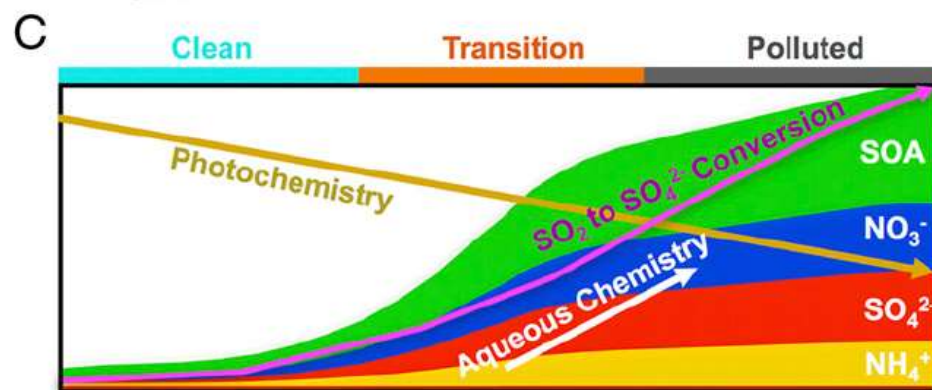
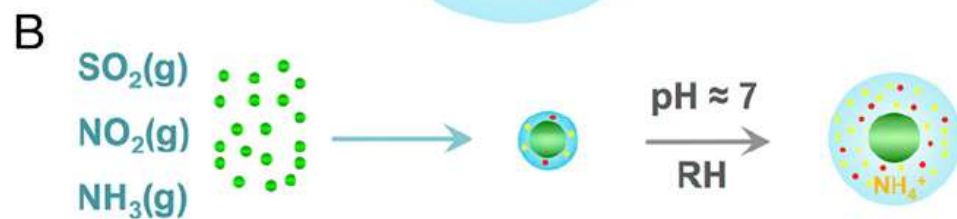
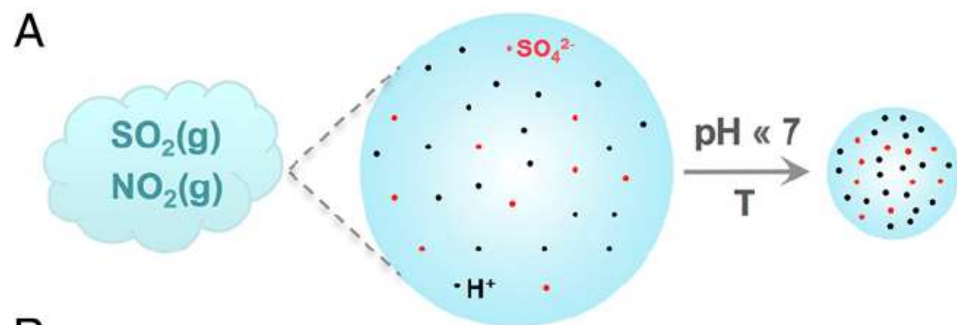
(2) 100 ppm SO₂/NO₂/NH₃ under different RH conditions for 1 hour

Measure the dry particle size before and after the reaction/ detect the chemical composition

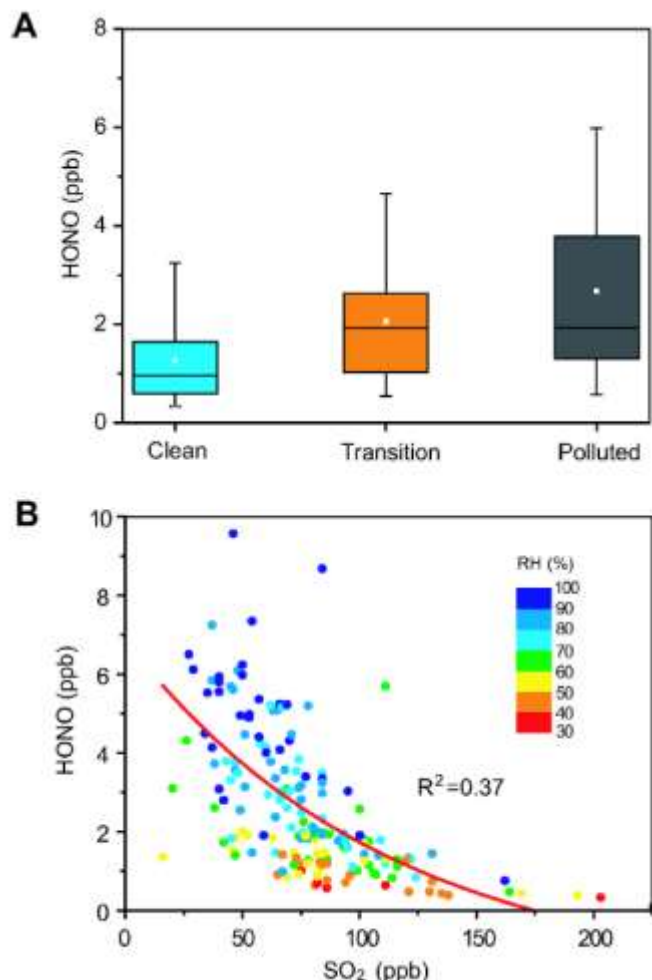
Size growth and sulfate signal can only be seen when seeds, SO₂, NO₂, NH₃ and high RH are all available for the reaction



London Fog vs Chinese Haze



“Persistent sulfate formation from London fog to Chinese haze”



Persistent sulfate formation from London Fog to Chinese haze

Gehui Wang^{1,2,3,4,5,6,7,8,9,10,11,12,13,14,15,16,17,18,19,20,21,22,23,24,25,26,27,28,29,30,31,32,33,34,35,36,37,38,39,40,41,42,43,44,45,46,47,48,49,50,51,52,53,54,55,56,57,58,59,60,61,62,63,64,65,66,67,68,69,70,71,72,73,74,75,76,77,78,79,80,81,82,83,84,85,86,87,88,89,90,91,92,93,94,95,96,97,98,99,100}, Renyi Zhang^{11,12}, Mario E. Gomez^{14,15}, Lingkai Yang^{16,17}, Miss Levy Zamora¹⁸, Min Hu¹⁹, Yan Lin²⁰, Jianfei Peng²¹, Song Guo²², Jingjing Meng²³, Jianjun Lu²⁴, Chanlei Chang²⁵, Tefeng Hu²⁶, Yanjun Ren²⁷, Yuesi Wang²⁸, Jiao Gao²⁹, Junli Cao³⁰, Zhibang An³¹, Wujun Zhou^{32,33}, Guohui Lin³⁴, Jinyuan Wang³⁵, Pengfei Tian³⁶, Wilmarie Mamerito-Ortiz³⁷, Jeremiah Secrett³⁸, Zhuofei Du³⁹, Jing Zhang⁴⁰, Dongjie Zhang⁴¹, Limin Zhang⁴², Min Shao⁴³, Weiqiang Wang⁴⁴, Yao Huang⁴⁵, Yuan Wang⁴⁶, Yujiao Zhu⁴⁷, Yin Li, Jiaxi Hu, Bowen Pan⁴⁸, Li Cai⁴⁹, Yuting Cheng⁵⁰, Yueyang Ji⁵¹, Fang Zhang⁵², Daniel Rosenfeld⁵³, Peter S. Liu⁵⁴, Robert A. Duco⁵⁵, Charles E. Kolb⁵⁶, and Mario J. Molina^{57,58}

¹State Key Laboratory of Loess and Quaternary Geology, Institute of Earth Environment, Chinese Academy of Sciences, Xi'an 710061, China; ²Key Laboratory of Aerosol Chemistry and Physics, Institute of Earth Environment, Chinese Academy of Sciences, Xi'an 710061, China; ³Department of Atmospheric Science, Texas A&M University, College Station, TX 77843; ⁴Department of Chemistry, Texas A&M University, College Station, TX 77843; ⁵School of Geographic Sciences, East China Normal University, Shanghai 200062, China; ⁶State Key Joint Laboratory of Environmental Simulation and Pollution Control, College of Environmental Science and Engineering Peking University, Beijing 100871, China; ⁷Department of Chemistry and Biochemistry, Florida International University, Miami, FL 33199; ⁸School of Environmental Science and Engineering, Shandong University, Jinan 250100, China; ⁹University of Chinese Academy of Sciences, Beijing 100049, China; ¹⁰Institute of Atmospheric Physics, Chinese Academy of Sciences, Beijing 100026, China; ¹¹Chinese Research Academy of Environmental Science, Beijing 100000, China; ¹²Nanjing Normal University, Beijing 100075, China; ¹³Xi'an Jiaotong University, Xi'an 710049, China; ¹⁴Key Laboratory for Severe-Weather Climate Change of the Ministry of Education, College of Atmospheric Science, Lanzhou University, Lanzhou 730000, China; ¹⁵State Key Laboratory for Structural Chemistry of Unstable and Stable Species, Institute of Chemistry, Chinese Academy of Sciences, Beijing 100086, China; ¹⁶Beijing National Laboratory for Molecular Science, Institute of Chemistry, Chinese Academy of Sciences, Beijing 100086, China; ¹⁷San Joaquin Laboratory, California Institute of Technology, Pasadena, CA 91125; ¹⁸Key Laboratory of Marine Environmental Science and Ecology, Ministry of Education, Ocean University of China, Qingdao 266100, China; ¹⁹School of Electrical Engineering, Wuzhen University, Wuzhen 310022, China; ²⁰School of Environmental Science and Engineering, Institute of Environmental Health and Pollution Control, Guangdong University of Technology, Guangzhou 510006, China; ²¹Program of Atmospheric Science, Institute of Earth Science, The Hebrew University of Jerusalem, Jerusalem 91904, Israel; ²²School of Environmental Science, University of East Anglia, Norwich, NR4 7TJ, United Kingdom; ²³Aerodyne Research, Inc., Billerica, MA 01821-5070 and Department of Chemistry and Biochemistry, University of California, Berkeley, La Jolla, CA 92092

Contributed by Mario J. Molina, October 9, 2016 (sent for review July 8, 2016); reviewed by Zhenqing Li and Saba Madhavi

Sulfate aerosols exert profound impacts on human and ecosystem health, weather, and climate, but their formation mechanism remains uncertain. Atmospheric media consistently underestimate sulfate levels under diverse environmental conditions. From atmospheric measurements in two Chinese megacities and complementary laboratory experiments, we show that the aqueous oxidation of SO₂ by NO₂ is key to efficient sulfate formation, not only feasible under two atmospheric conditions on fine aerosol with high relative humidity and NH₃ neutralization or under cloud conditions. Under polluted environments, the SO₂ oxidation process leads to large sulfate production rates and precise formation of inorganic and organic matter on aqueous particle, exacerbating severe haze development. Effective haze mitigation is achievable by intervening in the sulfate formation process with enhanced NH₃ and NO₂ control measures. In addition to explaining the polluted episodes currently occurring in China and during the 1952 London Fog, this sulfate production mechanism is widespread, and our results suggest a way to tackle this growing problem in China and much of the developing world.

Significance

Increasingly high levels of fine particulate matter (PM) occur frequently in China, but the mechanism of severe haze formation remains unclear. From atmospheric measurements in two Chinese megacities and laboratory experiments, we show that the oxidation of SO₂ by NO₂ occurs efficiently in aqueous media under two polluted conditions: first, during the formation of the 1952 London Fog via in-cloud oxidation, and second, on fine PM with NH₃ neutralization during severe haze in China. We suggest that effective haze mitigation is achievable by intervening in the sulfate formation process with NH₃ and NO₂ emission control measures. Hence, our results explain the outstanding haze problem during the historic London Fog formation and elucidate the dominant mechanism of severe haze in China.

Introduction

Fine particulate matter (PM), which typically contains a complex mixture of inorganic and organic species, has important implications for several environmental issues (1–3). Presently, the mechanisms leading to PM formation remain uncertain, particularly under highly polluted conditions, hindering efforts in developing effective mitigation policies to reduce their local, regional, and global impacts (1). It is well established, though, that sulfate (SO₄²⁻) is ubiquitous and is a key PM constituent in the atmosphere. Moreover, hygroscopic sulfate aerosols serve as efficient cloud condensation nuclei, affecting cloud formation, precipitation, and climate (4–8). A major fraction of regional acid deposition is attributed to the sulfate content that exerts debilitating effects on acid-sensitive ecosystems (9). Furthermore, high levels of fine PM have been implicated in adverse human health issues (1), as exemplified by high fatality during the 1952 London Fog (1, 10). Sulfur compounds are emitted globally from many natural and anthropogenic sources (1–3, 11),

1820-1105 • PNAS | November 23, 2016 | vol. 113 | no. 48

www.pnas.org/cgi/doi/10.1073/pnas.1604901113

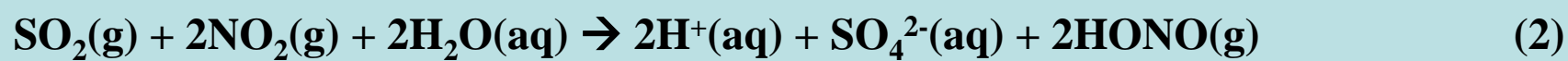
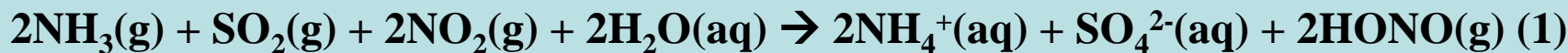
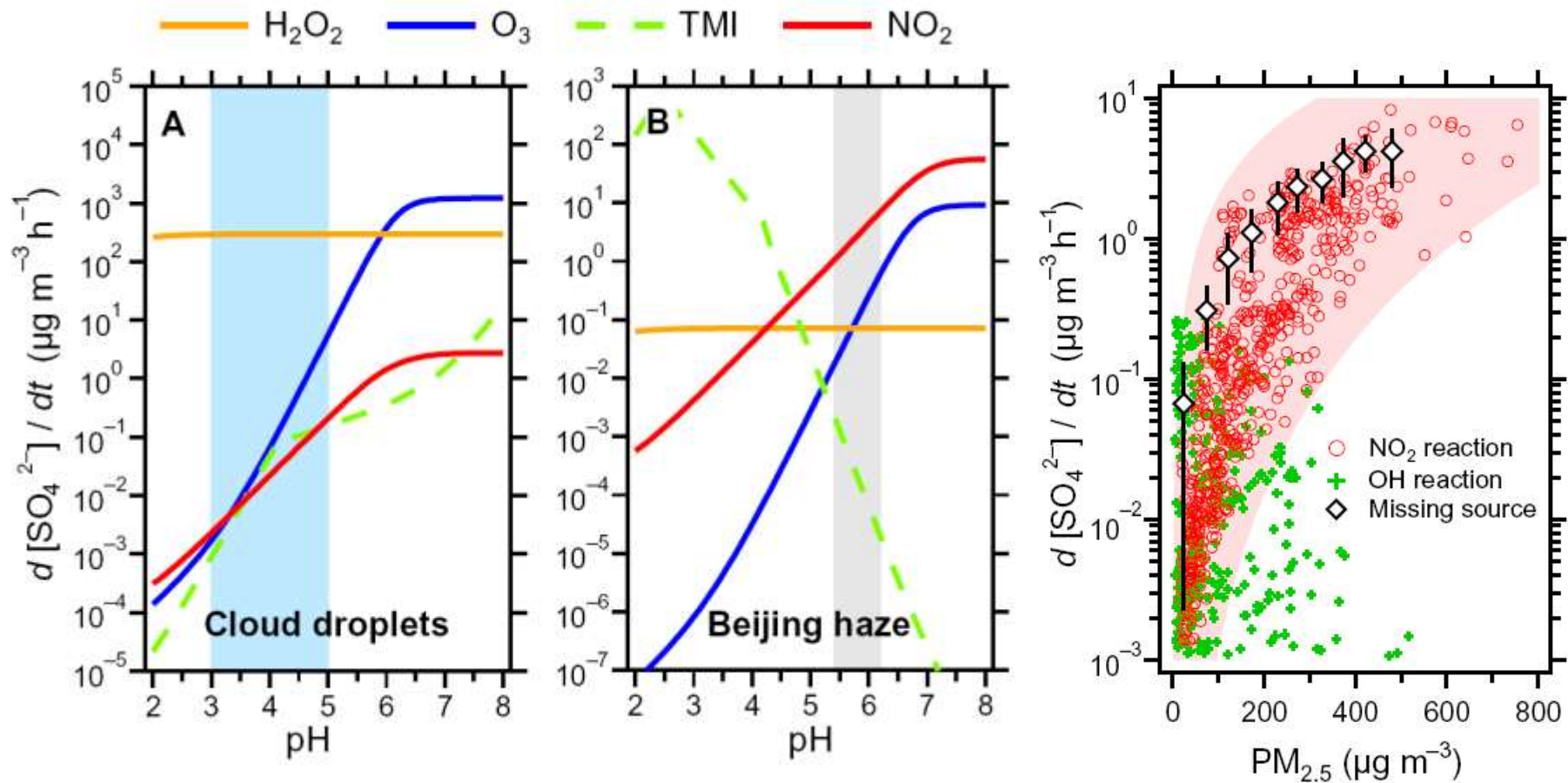


Table S5. Uptake coefficient (γ) of SO₂ on aerosols during Beijing 2015

	Average [SO ₄ ²⁻] ($\mu\text{g m}^{-3}$)	RH (%)	<i>N</i> ($\times 10^4$) (cm^{-3})	Average <i>D_p</i> (nm)	<i>S</i> ($\times 10^{-5}$) ($\text{cm}^2 \text{cm}^{-3}$)	[SO ₂ (g)] (ppb)	<i>d</i> [SO ₄ ²⁻] ($\mu\text{g m}^{-3}$)	<i>dt</i> (hr)	$\gamma \pm 1\sigma$
Clean	4	21	7.5	75.0	1.3	16.3	3.0	7.2	$(1.6 \pm 0.7) \times 10^{-5}$
Transition	14	41	9.0	114.2	3.7	24.2	12.7	6.0	$(2.1 \pm 1.6) \times 10^{-5}$
Polluted	26	56	8.1	116.2	3.4	16.2	14.7	7.0	$(4.5 \pm 1.1) \times 10^{-5}$

Table S6. Uptake coefficient (γ) of SO₂ on oxalic acid particles in the reaction chamber

RH (%)	<i>D_o</i> (nm)	<i>D_p</i> / <i>D_o</i>	<i>N</i> (cm^{-3})	<i>S</i> ($\times 10^{-5}$) ($\text{cm}^2 \text{cm}^{-3}$)	[SO ₂ (g)] (ppb)	<i>dt</i> (min)	$\gamma \pm 1\sigma$
30	45	1.06	1.0×10^3	1.3	250	60	$(6.7 \pm 9.1) \times 10^{-6}$
65	45	1.5	1.0×10^3	4.0	250	60	$(8.3 \pm 5.7) \times 10^{-5}$
70	45	2.31	1.0×10^3	3.4	250	60	$(3.9 \pm 1.2) \times 10^{-4}$



Cheng et al., Science Advances (2016)

Max Plank Institute of Chemistry: Dr. Chen et al using WRF-CMAQ model to simulate the aqueous production of SO_4^{2-} , demonstrating the most important role of SO_2 oxidation by NO_2 in Beijing haze formation process

Thank you for your attention !